

Spectrophotometry and Electrochemistry of Brilliant Blue FCF in Aqueous Solution of NaX

Bogdan Tutunaru*, Cristian Tigae*, Cezar Spînu, Ioana Prunaru

University of Craiova, Faculty of Sciences, Department of Chemistry, Calea București 107i, Craiova, România

*E-mail: tutunaruchim@yahoo.com, ctigae@yahoo.com

Received: 7 September 2016 / Accepted: 19 November 2016 / Published: 12 December 2016

The study of the electrochemical behaviour of Brilliant Blue FCF (BBfcf) food additive have been carried out by cyclic voltammetry on platinum electrode in aqueous solution of $0.1 \text{ mol}\cdot\text{L}^{-1}$ NaX (X = SO_4^{2-} , F⁻, Cl⁻, Br⁻, I⁻). The effect of counter anion on the electrochemical behavior of BBfcf was also investigated by electrochemical impedance spectroscopy (EIS). Electrochemical degradation rate of coloring food dye under constant current electrolysis was determined in the presence of various counter anions by UV-Vis spectrophotometry and obeyed the following order: $\text{I}^- < \text{SO}_4^{2-} < \text{F}^- < \text{Cl}^- < \text{Br}^-$. Kinetic first order was successfully applied to the experimental results in order to calculate the constant rate and the half-time for the electrochemical degradation process. Based on experimental data the mechanism for complete electrochemical mineralization is proposed.

Keywords: E133 food additive, electrodegradation, active species, degradation mechanism

1. INTRODUCTION

The increase of human population and rapid industrialization are two of the most important factors for the exploitation of natural water resources and their pollution. Brilliant Blue FCF (BBfcf) is a textile and food additive with IUPAC name: ethyl - [4 - [[4 - [ethyl -(3 - sulfophenyl) methyl] amino] phenyl] - (2 - sulfophenyl) methylidene] - 1 - cyclohexa - 2, 5 - dienyldene] - [(3 - sulfophenyl) methyl] azanium. Other similar name are: *FD&C Blue No.1*, *E133*, *Acid Blue 9*, *D&C Blue No. 4*, *Alzen Food Blue No. 1*, *Atracid Blue FG*, *Blue #1 Lake*, *Erioglaucine*, *Eriosky blue*, *Patent Blue AR*, *Xylene Blue VSG*, *C.I. 42090 Basacid Blue 755*, *Sulfacid Brilliant Blue 5 J*, *Neolan Blue E-A*.

The major use of BBfcf is as toilet cleaners, in paper industry, as agricultural marker, component of inks, as textile dye, indicator dye, biological stain, in pet food, beverages or

pharmaceuticals. Brilliant Blue FCF presents a very low acute and chronic toxicity; the genotoxic studies on mammals showed that is not toxic [1].

U.S. Food and Drug Administration (FDA) has accepted BBfcf as a additive for food, cosmetics and drugs with an acceptable daily intake (ADI) for humans of 12.0 mg/(kg body weight).

Recently, have been prepared a paper-based sensor for monitoring sun exposure. Under sun light, the food dye is degraded by employing titanium dioxide as photocatalyst resulting in gradual discoloration of the film [2]. The amyloid- β oligomers are neurotoxic species correlated with the onset of Alzheimer disease. Comparative studies showed that brilliant Blue G, R, FCF and Fast Green FCF interacts with amyloid- β oligomers reducing their cytotoxicity. By reducing the levels of these neurotoxic species, can block the progression of Alzheimer disease [3]. Brilliant Blue FCF is easily visible in the soil; is readily mobile and nontoxic; properties which make it an ideal color tracer for staining flow paths of water in soil [4].

Multi-walled carbon nanotube paste carbon electrode was used for quantitative determination of BBfcf and Tartrazine in soft drinks. Voltammertic methods have been used for simultaneous determination of these compounds with a low detection limit (nanomolar scale) [5]. Cathodic stripping voltammetry has been successfully applied to qualitative and quantitative determination of Brilliant Blue FCF in binary mixture with erythrosine and quinoline yellow in commercial food products [6]. Determination of E133 has been made with a new composite multi-walled carbon nanotube - graphite oxide - room temperature ionic liquids - modified glassy carbon electrode. This electrode was used for E133 determination from beverages with a detection limit of $3.01 \mu\text{g}\cdot\text{kg}^{-1}$ [7]. A new simple and sensitive electrochemical detection for electrophoretic analysis of food additives was developed. Brilliant Blue FCF was determined with a detection limit between 1.0 and $5.0 \text{ nmol}\cdot\text{L}^{-1}$ [8].

The effects of operational parameters such as pH, contact time, temperature and dye concentration were studied in the case of Brilliant Blue FCF removal by sorption on unmodified natural clay and modified with iron chloride [9]. The removal of Brilliant Blue FCF from aqueous solution, by sorption on Fe-zeolitic tuff was characterized by scanning electron microscopy, IR spectroscopy and X-ray diffraction [10]. The municipal wastewaters and Brilliant Blue FCF were photocatalytic degraded using Ag-doped ZnO particles [11]. New electrodes of multi-walled carbon nanotube functionalized with Brilliant Blue were synthesized on glassy carbon electrode and indium tin oxide for the determination of hydrogen peroxide [12]. A Brilliant Blue FCF-modified Nafion-coated electrode was developed for L-cysteine determination with high sensitivity ($111 \text{ nA}\cdot\mu\text{mol}\cdot\text{L}^{-1}$) and low detection limit ($0.5 \mu\text{mol}\cdot\text{L}^{-1}$) [13].

Small concentrations of synthetic dye deteriorates the quality of water and makes it unsafe for further use. Many chemical, physical, biological and physico-chemical methods have been used for pollutants removal [14-45]. Thus, in our previous studies we successfully investigated the stability of some compounds using electrochemical methods in tandem with UV-Vis spectrophotometry. The pesticides such as metribuzin were studied on bismuth electrode [21]. Electrochemical stability of certain drugs such as metronidazole [22] and benzocaine [23], a local anesthetic was investigated on thallium/ platinum electrode [22] and on an electrode based on poly-hematoxylin film electrodeposited on platinum electrode [23]. Other pharmaceutical compounds of the type hematoxylin [24] and sulfacetamide [25] were tested in terms of electrochemical stability on the carbon steel electrode, in

order to be useful as corrosion inhibitors for this alloy in the environment of sodium nitrate [24] and hydrochloric acid [25], respectively. The following dyes: Methylene Blue, Methyl Blue [26] and Methylorange [27] were electrodegraded on platinum electrode, their decomposition reaction respecting the first order kinetics.

This research shows an application of electrochemical methods to study electron transfer processes that occur at the interface metal / electrolyte solution containing the food additive Brilliant Blue FCF. Cyclic voltammetry (CV), electrochemical impedance spectroscopy (EIS) and UV-Vis spectrophotometry were performed on platinum electrode in BBfcf containing solution with different counter anions. The electrochemical degradation of Brilliant Blue FCF (BBfcf) from aqueous solution of NaX was investigated in order to identify the optimal experimental conditions to decrease the toxicity level of these wastewaters.

2. EXPERIMENTAL

2.1 Materials

Brilliant Blue FCF (E133; its molecular structure is presented in Figure 1) with food grade purity was obtained from a local commercial company. Other chemicals; Na₂SO₄, NaF, NaCl, NaBr and NaI were of analytical grade and used as received. Stock solutions represented by 100 mL of 10⁻³ mol·L⁻¹ food dye and 100 mL of 1.0 mol·L⁻¹ supporting electrolyte NaX (X = SO₄²⁻, F⁻, Cl⁻, Br⁻, I⁻) were prepared and kept in a dark environment at room temperature. Appropriate volumes of stock solutions BBfcf and NaX were diluted with distilled water to 100 mL. The working electrolyte solutions were represented by 2·10⁻⁵ mol·L⁻¹ BBfcf containing 0.1 mol·L⁻¹ supporting electrolyte NaX. A pH meter (Hanna Instruments) was employed for pH measurements.

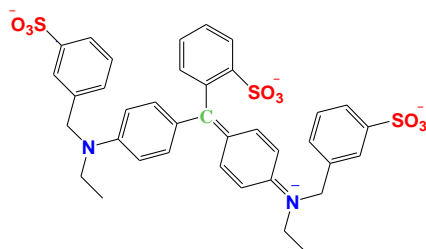


Figure 1. The molecular structure of BBfcf.

2.2. Methods

2.2.1. Cyclic voltammetry

The experiments were carried out with VoltaLab 40 electrochemical multifunctional workstation (model 40) equipped with VoltaMaster 4 software. Cyclic voltammograms were recorded in a three-electrode one-compartment electrochemical cell configuration. Working electrode and

auxiliary electrode were represented by platinum plates with an active area of 2 cm². All working potentials were recorded using Ag/AgCl, KCl_{sat} reference electrode. Cyclic voltammograms of Pt electrode in analyzed solutions were registered in the domain potential -1.5 V ÷ 2.0 V starting with an anodic direction, with a scan rate = 100 mV·s⁻¹.

2.2.2. Electrochemical impedance spectroscopy (EIS)

EIS spectra of Pt electrode in 2·10⁻⁵ mol·L⁻¹ BBfcf containing 0.1 mol·L⁻¹ supporting electrolyte NaX (X = SO₄²⁻, F⁻, Cl⁻, Br⁻, I⁻) were recorded at open circuit potential in the frequency domain 10⁵ Hz ÷ 10⁻² Hz. Impedance spectra were obtained with an AC voltage amplitude of 10 mV after 4.0 minutes of relaxation time.

2.2.3. Constant current electrolysis

Electrochemical degradation of BBfcf in the specified solutions by constant current electrolysis (50 mA·cm⁻²) was performed using the voltage/current source Keithley SourceMeter (model 2420 3A) accessorized with TestPoint software. In this case, all experiments were performed in a bi-electrode electrochemical cell configuration in dynamic regime of convection (stirring rate = 5 rotations·s⁻¹). Thermal regime of experimental conditions was room temperature (23 ± 1 °C).

2.2.4. Spectrophotometric analysis

BBfcf solutions freshly prepared and after different times of electrolysis were analyzed by UV-Vis spectrophotometry using a Varian Cary 50 spectrophotometer, with CaryWin UV software. Thereby, at constant intervals of time, volumes of 4 mL were collected in a spectrophotometric quartz cuvette and were recorded the UV-Vis spectra at wavelengths ranging between 800 and 200 nm.

3. RESULTS AND DISCUSSION

3.1 Cyclic voltammetry

Cyclic voltammograms of platinum electrode in 0.1 mol·L⁻¹ sulfate solution, in the absence and in the presence of 2·10⁻⁵ mol·L⁻¹ E133 are shown in Figure 2. Cyclic voltammograms were recorded with an initial anodic sweep and a scan speed of 100 mV per sec. in potential range -1.5 V ÷ +2.0 V.

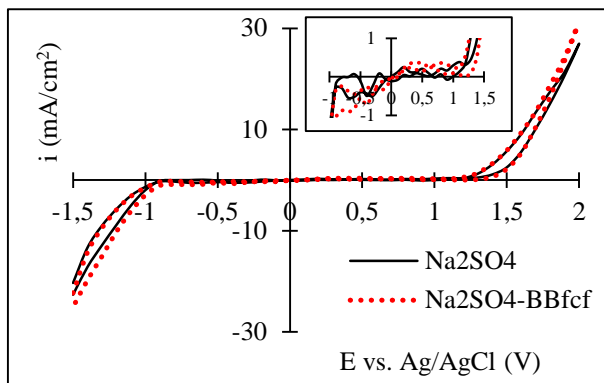
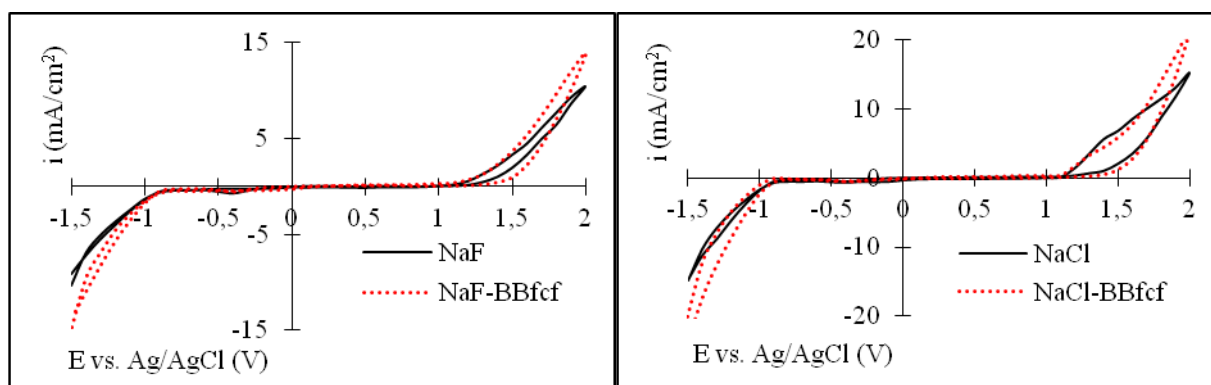


Figure 2. Cyclic voltammograms of Pt electrode recorded in: 0.1 mol·L⁻¹ Na₂SO₄ (black solid lines) and in 0.1 mol·L⁻¹ Na₂SO₄ in the presence of 2·10⁻⁵ mol·L⁻¹ BBfcf (red dotted lines).

Experimental results indicate a very small difference between the two voltammograms. At potential values greater than 1.8 V the current densities are higher in the presence E133; this is due to the oxidation of organic molecules of dye. Has been demonstrated, by density functional theory and linear sweep voltammetry, that sulfate adsorption on platinum electrode take place at potentials of 0.3 ÷ 0.45 V [46]. According to Figure 2 (insert detail), current density peaks can be observed, peaks which are attributed to sulfate adsorption (0.3 ÷ 0.45 V) and phase transition of ordered / disordered sulfate adlayer (~0.7 V) [46-48]. At potential values around 0.0 V, the registered current densities can be attributed to hydrogen adsorption / desorption process [49, 50], while the peaks observed at higher values of working potentials (0.7 ÷ 1.1 V) are due to oxygen adsorption [50, 51]. Literature data presents that the potential domain 0.5 ÷ 1.35 V also corresponds to Pt-oxide, Pt-hydroxide species formation [51-53]. In the presence of BBfcf molecules, the current density values are higher which demonstrate that the electrochemical processes take place by adsorption of organic molecules on platinum surface. Similar results are also recorded if the fluoride ions are present in the electrolyte solution. When chloride or bromide anions are used, the recorded anodic and cathodic current densities in the presence of dye are obviously higher compared to the case of simple supporting electrolyte (Figure 3).



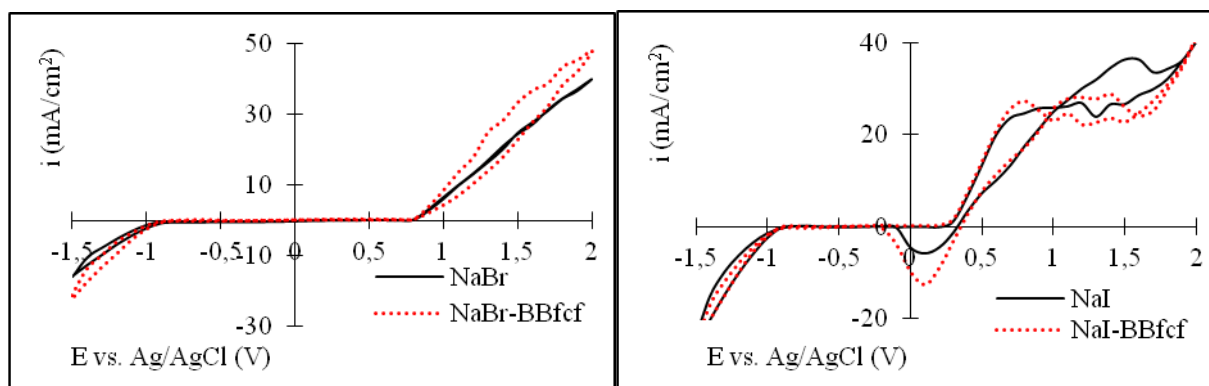
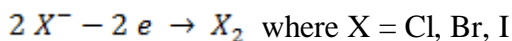


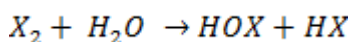
Figure 3. Cyclic voltammograms of Pt electrode recorded in: $0.1 \text{ mol}\cdot\text{L}^{-1}$ NaX (black solid lines) and in $0.1 \text{ mol}\cdot\text{L}^{-1}$ NaX in the presence of $2\cdot 10^{-5} \text{ mol}\cdot\text{L}^{-1}$ BBfcf (red dotted lines), (X= F, Cl, Br, I).

If the electrolysis takes place in the presence of sulfate or fluoride anions, the electrochemical degradation occurs through a direct mechanism; the supporting electrolyte does not participate in the electrode processes, being considered an inert electrolyte. When the electrochemical degradation of the E133 is carried out in the presence of Cl, Br or I anions, the mechanism of electrochemical degradation is an indirect one because the supporting electrolyte participates to electrode processes. In these cases, the electrode processes are accompanied by the discharge of halide anions with the formation of the corresponding halogen molecule.



Knowing that the standard potential of F^-/F_2 redox couple has a value of 2.87 V, it is impossible for the fluoride anions to participate at the electrode processes. In the case of Cl^- , Br^- and I^- anions, the corresponding standard potentials presents values ranging between 1.0 and 1.4 V, and consequently the halogen molecules are generated at the electrode / electrolyte interface [54-56]. The experimental observations are the result of synergistic effects and can not be attributed to one individual process.

In the aqueous electrolyte solution, the halogen molecules formed to the surface of the electrode reacts with the water molecules, according to the reaction:



These reactions are responsible for the appearance of corresponding oxygenated anions (ClO^- - hypochlorite, BrO^- - hypobromite, IO^- - hypiodite); these anions have an oxidizing action. Thus, the dye molecule supports a heterogeneous oxidation process, direct to the electrode surface and a homogeneous oxidation process, indirectly by oxyhalogenated anions.

3.2 Electrochemical impedance spectroscopy

For a better understanding of the processes occurring at the metal-solution interface there were made electrochemical impedance spectroscopy (EIS) measurements. The electrochemical system was perturbed with a sinusoidal voltage of 10 mV amplitude and variable frequencies ranging between $10^5 \text{ Hz} \div 10^{-2} \text{ Hz}$. These experiments were performed with fresh solutions and clean surfaces of platinum working electrode. In Figure 4 are plotted the experimental data obtained by means of

impedance measurements: $-Z_i$, Z_r , $\log(\text{Frequency})$, $\log(Z)$ and Phase as complete 3D Nyquist and 3D Bode diagrams for Pt electrode in $0.1 \text{ mol}\cdot\text{L}^{-1} \text{ Na}_2\text{SO}_4$ in the absence and in the presence of $2\cdot 10^{-5} \text{ mol}\cdot\text{L}^{-1} \text{ BBfcf}$. 3D Nyquist plots are characterized by a linear dependence, characteristic to an inert electrode. Solution resistance is often a significant factor that influence the impedance value. The resistance of an electrolyte solution depends on the ions concentration, nature of ions, temperature, and the geometry and area of the electrode in which current is carried [57].

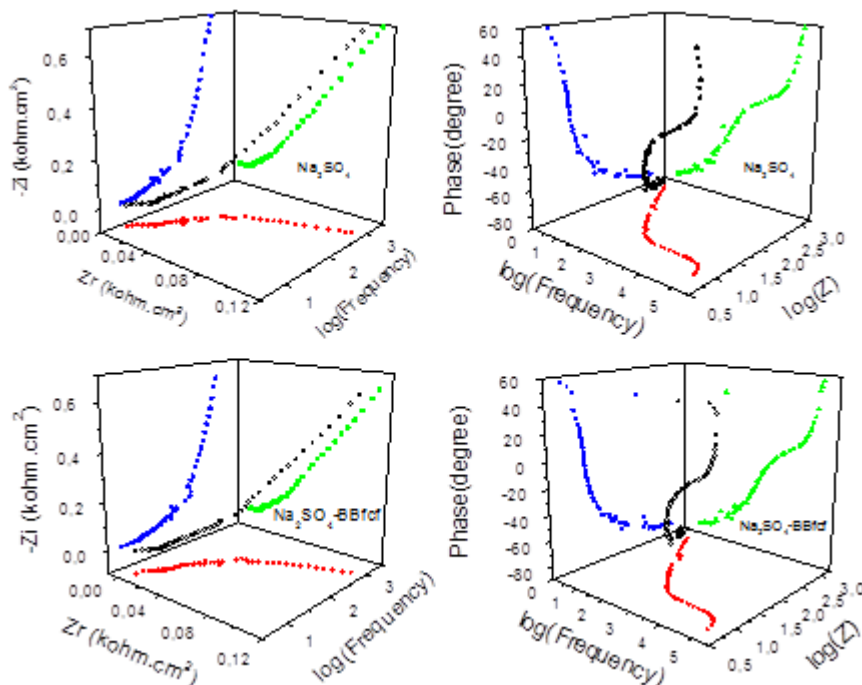


Figure 4. 3D Nyquist and 3D Bode diagrams of Pt electrode obtained in $10^{-1} \text{ mol}\cdot\text{L}^{-1} \text{ Na}_2\text{SO}_4$ solution in the absence and in the presence of $2\cdot 10^{-5} \text{ mol}\cdot\text{L}^{-1} \text{ BBfcf}$.

Table 2 shows the electrochemical parameters obtained from impedance measurements; R_s - solution resistance ($\Omega\cdot\text{cm}^2$) and C_{dl} – double layer capacitance ($\mu\text{F}\cdot\text{cm}^{-2}$).

Table 2. Electrochemical parameters obtained from impedance measurements.

Electrolyte	R_s $\Omega\cdot\text{cm}^2$	C_{dl} $\mu\text{F}\cdot\text{cm}^{-2}$
$\text{Na}_2\text{SO}_4 / \text{Na}_2\text{SO}_4+\text{E}-133$	16.2 / 13.3	14.3 / 3.6
$\text{NaF} / \text{NaF}+\text{E}-133$	43.3 / 25.0	1.9 / 13.9
$\text{NaCl} / \text{NaCl}+\text{E}-133$	29.2 / 14.9	2.5 / 1.2
$\text{NaBr} / \text{NaBr}+\text{E}-133$	25.3 / 16.2	15.8 / 27.1
$\text{NaI} / \text{NaI}+\text{E}-133$	17.6 / 12.8	756.7 / 370.9

It is observed a decrease of the electrolyte resistance values with the addition of additive in the electrolyte solution; this decrease being more evident in the case of fluoride ions (Figure 5).

Because the electrode surface and the distance between the electrodes remains the same in each experiment, the decrease of double layer capacity is due to a lower permittivity. The measure of the double layer capacity corresponds to the concentration of the adsorbed ions and the electrodes surface. As the molecules are more polar or more polarizable, there is an increase of forces that lead to the accumulation of these molecules in the double layer.

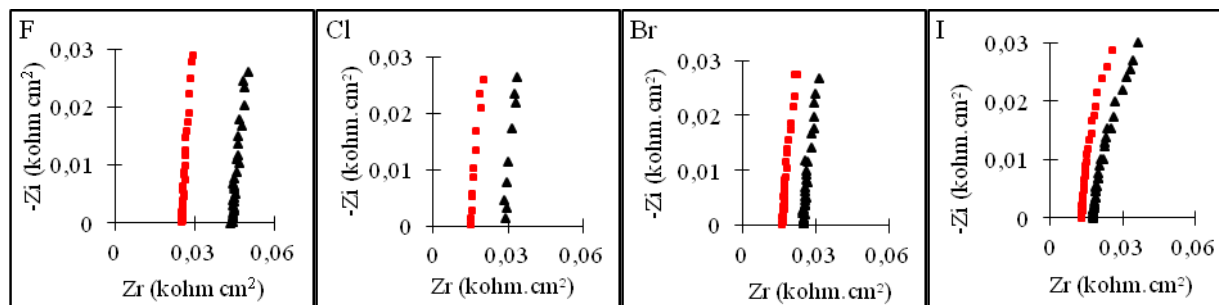


Figure 5. The Nyquist diagrams of Pt electrode obtained in: a - 10^{-1} mol·L $^{-1}$ NaX (X – F, Cl, Br, I) solution in the absence and in the presence of $2 \cdot 10^{-5}$ mol·L $^{-1}$ BBfcf.

Not all processes are heterogeneous due to chemical reactions that take place in the electrolyte solution. This complicates the description of the whole system capacity of the electrode-electrolyte phase interface. It can be observed a noticeable decrease of double layer capacity due to an increase of permittivity. If the electrolyte solution contains fluoride anions or bromide, then double layer capacitance increases. The increase of permittivity values, in this case, is correlated to an increase of organic molecules polarity. The increase of the charge molecule allows it to participate more easily in the electrode processes. The difference between the two cases is due to the fact that the fluoride ions are inert, while the bromide ions participate to the electrode processes. The permittivity value depends on the surface charge density; its value decreases with charge density increasing [58]. Fluoride anions presents the highest electronegativity; the increase of permittivity value can be explained by a higher level of dipoles ordering [57, 58].

The results obtained by electrochemical impedance measurements are in agreement with those obtained by cyclic voltammetry.

3.3 UV-Vis spectrophotometry / Kinetics of the process

Electrochemical behaviour of BBfcf in aqueous solutions of NaX was analyzed by UV-Vis spectrophotometry. UV-Vis spectra of aqueous solutions containing $2 \cdot 10^{-5}$ mol·L $^{-1}$ BBfcf, 0.1 mol·L $^{-1}$ Na_2SO_4 were recorded at different times: 10 min.; 20 min.; 30 min.; 40 min.; 50 min. and 60 min., at wavelengths between 200-800 nm (Figure 6).

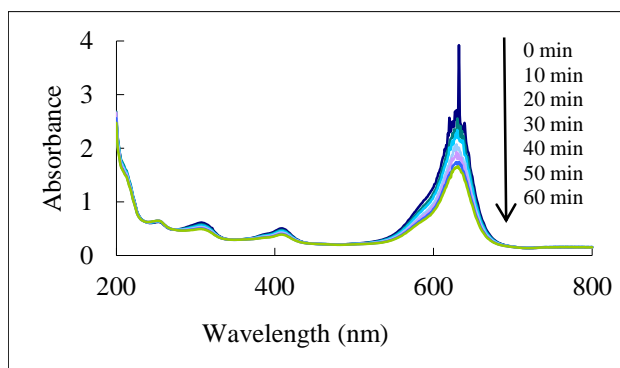
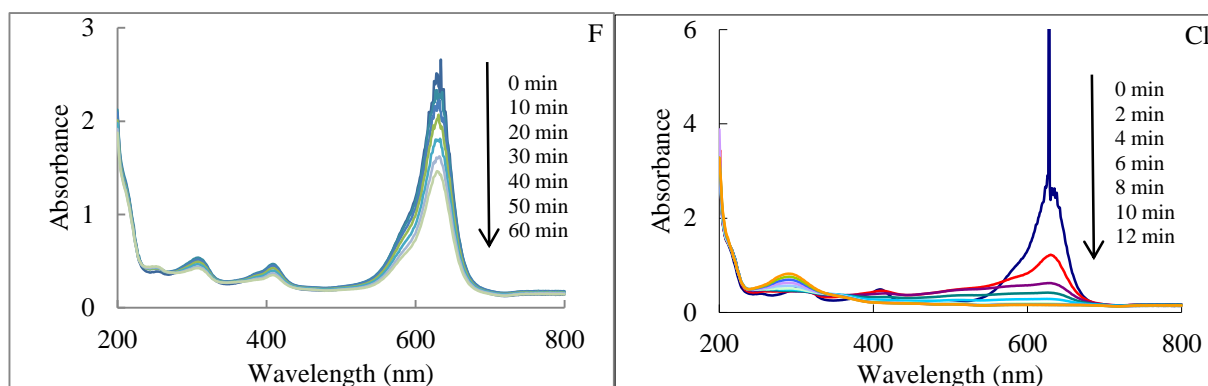


Figure 6. UV-Vis spectra of the solution containing $2 \cdot 10^{-5} \text{ mol} \cdot \text{L}^{-1}$ BBfcf $0.1 \text{ mol} \cdot \text{L}^{-1}$ Na_2SO_4 at different times of electrolysis.

Before the start of the electrolysis process, there are identified four absorption maxima in the absence of halide anions; three in UV range of wavelengths (255 nm, 308 nm, 409 nm) and one in the Vis domain (630 nm) (Figure 6). While the current passing through the electrolyte solution, it is observed a decrease of the intensities for all absorption maxima. Consequently the dye concentration decreases, due to its degradation at the electrode surface. The charge transfer processes at the electrode surface are accompanied by a slow degradation of both chromophore and auxochrome groups. In the presence of sulfate ions in the electrolyte solution, the dye molecule is degraded in a low ratio. Quantitative assessment of the organic molecules degradation is expressed by Degradation Degree (DD %) given by the following equation: **Degradation Degree (DD %)** = $\frac{A_0 - A_t}{A_0} \cdot 100$; where A_0 is the initial absorbance value before starting the electrolysis; A_t represents the absorbance value recorded at a time “t” of electrolysis; (A_0 and A_t corresponds to the wavelength value of 630 nm).

The degradation degree in the presence of sulfate ions, reach a maximum of 41 % after one hour of electrolysis (Figure 8).

A similar phenomenon is also observed in the presence of fluoride ions (Figure 7). In this case the degree of degradation is slightly higher, reaching a value of about 52 % after 60 minutes of electrolysis. The higher value of DD (~ 11 %) obtained in the presence of fluoride anions can be attributed to a stronger interaction of dye molecule with the fluoride ions; greater polarization / polarizability can lead to a higher degree of degradation.



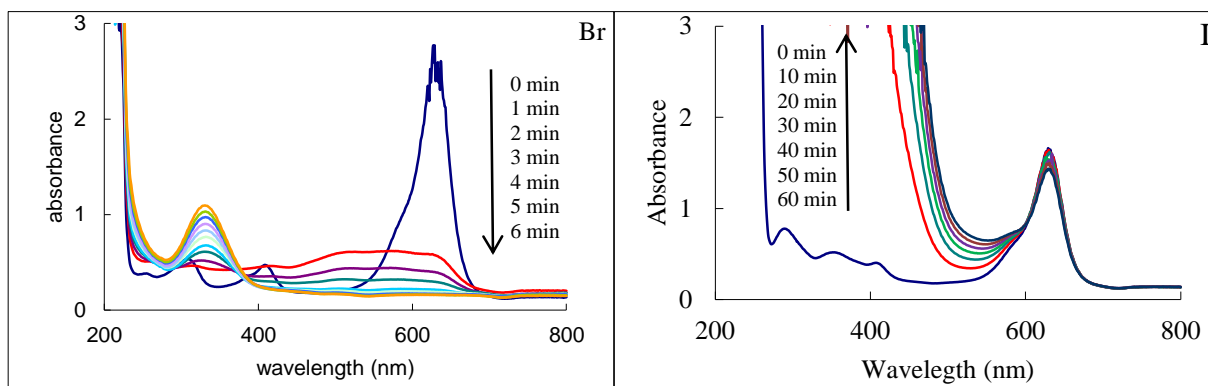


Figure 7. UV-Vis spectra of the solution containing $2 \cdot 10^{-5} \text{ mol}\cdot\text{L}^{-1}$ BBfcd, $0.1 \text{ mol}\cdot\text{L}^{-1}$ NaX (X = F, Cl, Br, I) at different times of electrolysis.

The presence of chloride and bromide ions presents a similar pathway for electrochemical degradation of BBfcd molecules (Figure 7). In these cases the spectrophotometric scans are performed at much lower period of time; every two minutes in the case of Cl^- ions and every minute for Br^- ions.

Electrochemical degradation of dye molecule is 100 % in just 5 minutes (in the presence of Br ions) and in 12 minutes (in the presence of Cl ions). Electrochemical degradation of dye molecule is complete (DD = 100 %) in the presence of Br and Cl ions in very short times of 5 minutes and 12 minutes respectively.

The shapes of spectrophotometric scans recorded in the presence of different anions indicates the existence of different mechanisms for BBfcd degradation; i) a similar mechanism can be predicted for BBfcd electrochemical degradation in the presence of sulfate and fluoride anions, ii) the degradation pathway in the presence of chloride ions is analogous to that in the presence of bromide ions, iii) iodine ions favors the electrochemical degradation of auxochrome groups without affecting the structure of the chromophore system.

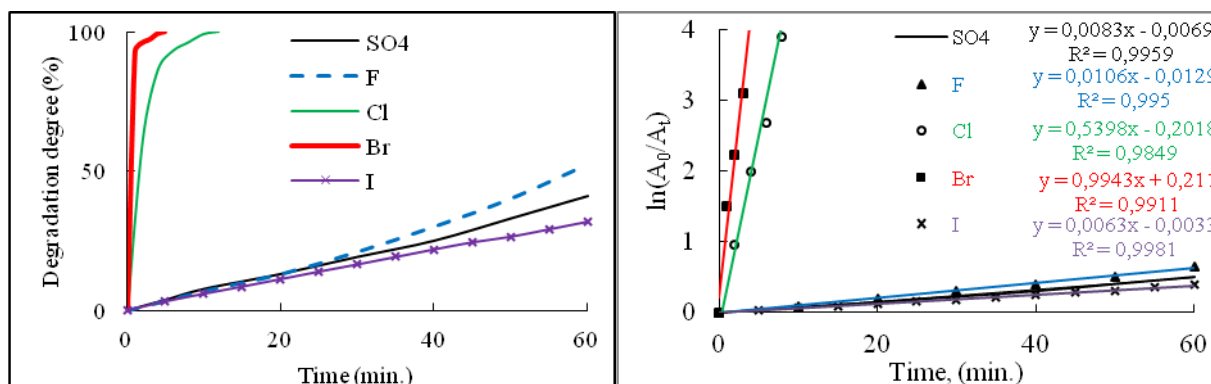


Figure 8. Time variation of degradation degree and first order kinetics simulation data.

As can be seen from Figure 8 the degradation degrees are influenced by the presence of different anions in the following order: $\text{I} < \text{SO}_4 < \text{F} < \text{Cl} < \text{Br}$. Similar results for textile dye Brilliant Blue FCF degradation are reported [59-61]. Oxidative degradation of BBfcd in aqueous solution was investigated using the Fenton reaction [59]. The study of experimental parameters indicates: i) in the

concentration range $5 \cdot 10^{-6} \text{ mol}\cdot\text{L}^{-1}$ to $10^{-4} \text{ mol}\cdot\text{L}^{-1}$ it was observed that while the concentration decrease, the degradation degree also decrease from 95 % to 10 % at the same reaction time; ii) the influence of Fe^{3+} concentration indicate a maximum value of degradation (95 %) at $2 \cdot 10^{-4} \text{ mol}\cdot\text{L}^{-1}$ Fe^{3+} ; if the concentration of ferric ions decrease to $10^{-5} \text{ mol}\cdot\text{L}^{-1}$ then the degradation efficiency was less than 10 %; iii) BBfcf degradation increased (from ~5 % to ~95 %) as the H_2O_2 concentration increased (from $10^{-4} \text{ mol}\cdot\text{L}^{-1}$ to $2 \cdot 10^{-3} \text{ mol}\cdot\text{L}^{-1}$) at 100 min.; iv) the addition of Orange II ($10^{-5} \text{ mol}\cdot\text{L}^{-1}$) to BBfcf solution ($5 \cdot 10^{-5} \text{ mol}\cdot\text{L}^{-1}$) results in degradation degree increase from 25 % to 60 % at 70 min.; v) BBfcf degradation degree in the presence of aromatic additives such as gallic acid, salicylic acid and 2-nitrophenol was 95 %, 87 % and 75 % respectively at 10 min..

Figure 8 shows the fitting of experimental data to kinetics model of first order reactions. Experimental results are simulated to first order kinetic model with a standard deviation close to the unit, which confirms that the electrochemical degradation processes occurring after first order kinetics. The kinetic parameters are listed in Table 1; rate constant (k), half-time ($t_{1/2}$) and the increment factor (α). The half-time is the time taken for the concentration of the dye to become half of its initial value while the increment factor represents a multiplication factor of k_{max} . Rate constant values obtained from electrochemical degradation ($0.006 \div 0.99 \text{ min}^{-1}$; Table 3) shows good agreement with those obtained by different experimental parameters ($0.0005 \div 0.23 \text{ min}^{-1}$) [59]. BBfcf degradation was monitored by high performance liquid chromatography and visible spectrometry in the presence of ascorbic acid (100, 250 and $500 \text{ mg}\cdot\text{L}^{-1}$) in acetate buffer solution (pH = 5.5) [60]. According to experimental results the rate of degradation increases with the concentration of the ascorbic acid.

Table 3. The kinetic parameters obtained by first-order simulation of experimental data.

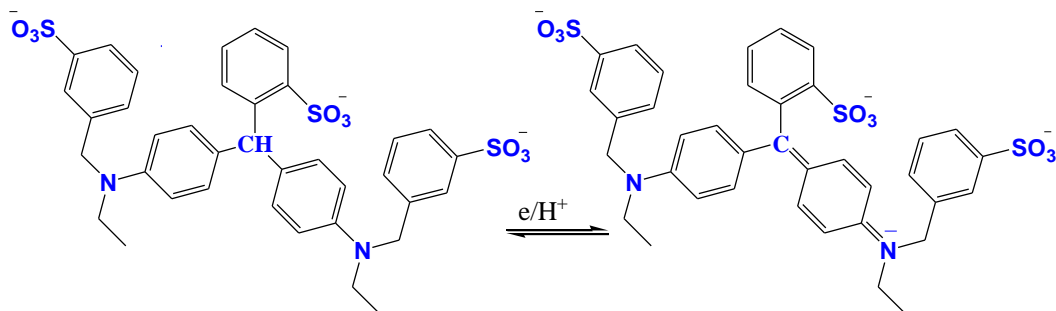
counter-anion	rate constant, k (min^{-1})	half-time, $t_{1/2}$ (min)	$\alpha = \frac{k}{k_{max}}$
SO_4^{2-}	0,0083	83,49	0.0083
F^-	0,0106	65,37	0.0107
Cl^-	0,5398	1,28	0.5460
Br^-	0,9943	0,69	1
I^-	0,0063	110	0.0063

According to experimental data, in the presence of bromide ions, is obtained the highest value of constant rate and the lowest value of half-time.

The electrolysis of BBfcf in the presence of NaX showed that the complete colour removal were only achieved using Cl^- and Br^- while in the presence of SO_4^{2-} , F^- and I^- only a partial oxidation of BBfcf molecule was performed.

3.4 Mechanism of electrochemical degradation

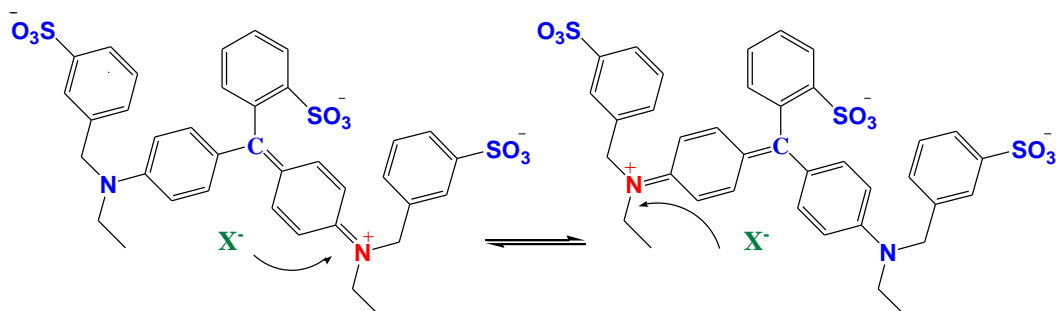
According to literature data [59-61] the molecule of BBfcf can dissociate in aqueous solutions due to its negative sulfonate groups / positive aminic groups by taking into consideration the following equilibrium between the related ionic structures (Scheme 1).



Scheme 1. The equilibrium of electrons/protons transfer for BBfcf molecule.

The degree of dissociation of the sulfonic and aminic groups is influenced by the pH and the nature of the anions present in the electrolyte solution. The pH value of 5.6 used in electrochemical measurements (pH-meter, Hanna Instruments) indicate that the dye molecule exists mainly in a neutral form. This value being very close to neutral pH, cannot be exclude the possibility that the molecule exists as mono- or bi-valent anionic forms.

In order to determine the mechanism of electrochemical degradation of BBfcf, must be taken into account the processes of protons/anions transfer, the coordinating processes, the electrostatic interactions and the associated equilibria of these processes that can exists in the electrolyte solution (Scheme 2).



Scheme 2. The interaction of the counter anion with the amino groups, and the corresponding mesomere structures.

The dye molecule contains more benzene rings as chromophore groups and more organic functionalities (sulfate and amine) as auxochrome groups. In Figure 9 are presented the spectrophotometric scans of $2 \cdot 10^{-5} \text{ mol} \cdot \text{L}^{-1}$ BBfcf solution in the presence of $0.1 \text{ mol} \cdot \text{L}^{-1}$ NaX. In the presence of sulfate anion, the UV-Vis spectra presents three absorption maxima in the UV domain ($\epsilon_2 = 409 \text{ nm}$, $\epsilon_3 = 308 \text{ nm}$, $\epsilon_4 = 255 \text{ nm}$) and one absorption maximum in the Vis domain at $\epsilon_1 = 630 \text{ nm}$.

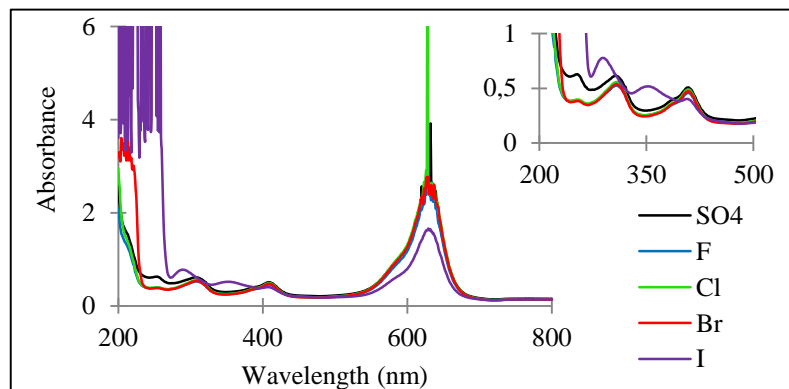
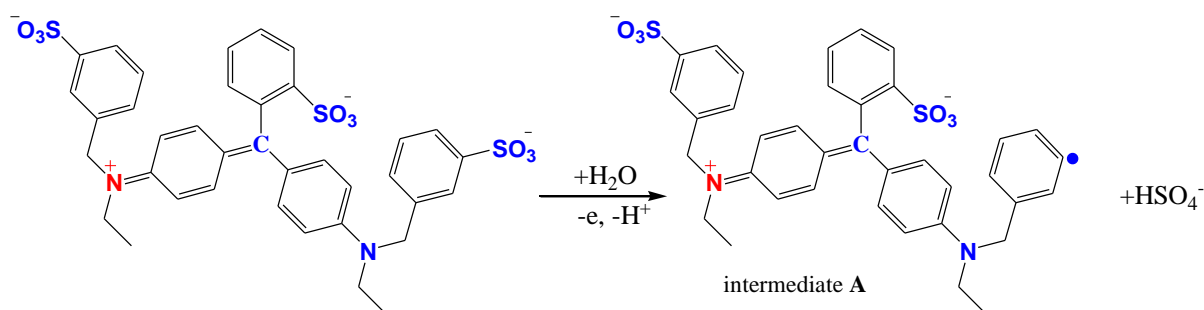


Figure 9. UV-Vis spectrophotometric curves of $2 \cdot 10^{-5} \text{ mol} \cdot \text{L}^{-1}$ BBfcf solution containing $0.1 \text{ mol} \cdot \text{L}^{-1}$ NaX ($X = \text{SO}_4^{2-}$, F^- , Cl^- , Br^- , I^-), before electrolysis.

In the presence of F^- , Cl^- and Br^- anions is registered a decrease in the intensity peaks at wavelengths of 308 nm and 255 nm, without modification of wavelengths values (insert of Figure 9). At the same time, the peak intensity recorded at the wavelength of 630 nm increases in the presence of chloride anions. It is obvious that the solute polarity/polarizability play an important role in the description of the solvatochromic effects observed in the studied electrolyte solutions. The solute–solvent interactions are more pronounced in the presence of iodide anions, by means of an rearrangement of the conjugated system. I^- anions determine a solvatochromic shifts of the UV molecular absorption bands registered at the wavelength values of $\epsilon_3 = 308 \text{ nm}$ and $\epsilon_4 = 255 \text{ nm}$. These absorption bands are attributed to an intramolecular charge transfer and supports a positive solvatochromism (bathochromic shift) with changing the solvent polarity ($\epsilon_3 = 308 \text{ nm} \rightarrow 355 \text{ nm}$ and $\epsilon_4 = 255 \text{ nm} \rightarrow 292 \text{ nm}$).

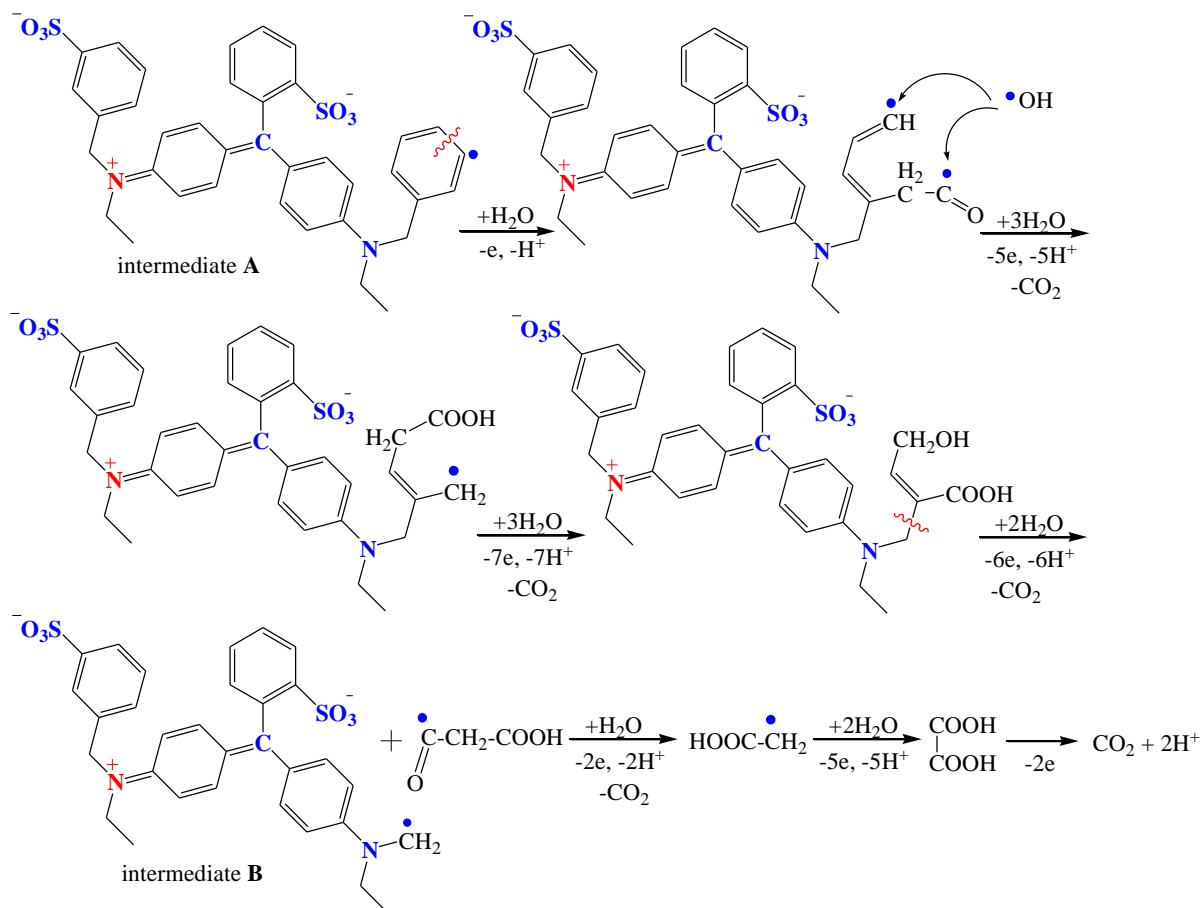
The first step of electrochemical degradation is the oxidative elimination of sulfonic group (Scheme 3).



Scheme 3. Mechanism for electrooxidative elimination of sulfonic group.

Sulfate formation in the initial stage of oxidative degradation was also demonstrated [59-61]. After this step, a benzene radical is obtained (intermediate A); a reactive specie which participate in subsequent transfers of electrons and protons with benzene ring opening (Scheme 4). Intermediate A formation, in the initial stage of oxidative degradation, was demonstrated by liquid chromatography

and mass spectrometry [59-61]. To study the pathway of electrochemical degradation through reduction and/or oxidation reactions also involves the study of electrochemical behavior; the assessment of the functional groups reactivity; electron/protons transfer reactions and oxidative eliminations [62, 63]. Similar electrochemical degradations pathway has been reported for azo dye through successive oxidative cleavage of covalent bonds and eliminations yielding to final inorganic compounds [63].



Scheme 4. The mechanism for electrochemical mineralization of benzene ring.

Through successive and / or parallel steps, intermediate A is oxidized with gradual cleavage of C-C bonds to form some more or less stable species with mixed functionalities (alcohol, aldehyde). Carbon atoms are gradually electro-oxidated to higher oxidation states. The corresponding carboxylic acids are oxidative decarboxylated with elimination of carbon dioxide. After complete mineralization of benzene ring, intermediate B is obtained - another active radicalic specie having lower atomic weight.

Subsequent oxidation occurs on the nitrogen of the amino group; the nitrogen atom from intermediate B is removed as nitrogen dioxide (Scheme 5).

3. H. E. Wong, W. Qi, H. M. Choi, E. J. Fernandez and I. Kwon, *ACS Chem. Neurosci.*, 2 (2011) 645.
4. M. Flury and H. Fluhler, *J. Environ. Qual.*, 23 (1994) 1108.
5. S. M. Ghoreishi, M. Behpour and M. Golestaneh, *Anal. Methods*, 3 (2011) 2842.
6. M. Florian, H. Yamanaka, P. A. Carneiro and M. V. Zanoni, *Food Addit. Contam.*, 19 (2002) 803.
7. M. Wang, M. Yang, Q. Sun, Y. Gao and J. Zhao, *Int. J. Environ. Anal. Chem.*, 95 (2015) 969.
8. K. S. Lee, M. J. Shiddiky, S. H. Park, D. S. Park and Y. B. Shim, *Electrophoresis*, 29 (2008) 1910.
9. K. A. Hernandez-Hernandez, M. Solache-Rios and M. C. Diaz-Nava, *Water, Air, & Soil Pollution*, 224 (2013) 1562.
10. S. Pinedo-Hernandez, C. Diaz-Nava and M. Solache-Rios, *Water, Air, & Soil Pollution*, 223 (2012) 467.
11. T. Parvin, N. Keerthiraj, I. A. Ibrahim, S. Phanichphant and K. Byrappa, *Int. J. Photoenergy*, 2012, Article ID 670610 (2012) doi:10.1155/2012/670610.
12. Y. Li, C. Y. Yang and S. M. Chen, *Int. J. Electrochem. Sci.*, 6 (2011) 4829.
13. S. M. Chen, J. Y. Chen and R. Thangamuthu, *Electroanal.*, 20 (2008) 1565.
14. A. Biati, S. M. Khezri and A. M. Bidokhti, *Int. J. Environ. Res.*, 8 (2014) 653.
15. W. Balla, A. H. Essadki, B. Gourich, A. Dassaa, H. Chenik and M. Azzi, *J. Hazard. Mater.*, 184 (2010) 710.
16. V. K. Gupta, I. Ali, T. A. Saleh, A. Nayak and S. Agarwal, *RSC Adv.*, 2 (2012) 6380.
17. S. Deng, H. Xu, X. Jiang and J. Yin, *Macromolecules*, 46 (2013) 2399.
18. A. Idris, M. S. Suhaimi, N. A. M. Zain, R. Rashid and N. Othman, *Desalin. Water Treat.*, 52 (2014) 6694.
19. M. Zarei, A. Niaei, D. Salari and A. R. Khataee, *J. Electroanal. Chem.*, 639 (2010) 167.
20. A. Pirkarami, M. E. Olya and N. Yousefi Limaee, *Prog. Org. Coat.*, 76 (2013) 682.
21. A. Samide, B. Tutunaru, N. Cioatera, A. C. Vladu, C. Spinu and C. Tigae, *Chem. Eng. Commun.*, 2016, DOI:10.1080/00986445.2016.1168818.
22. B. Tutunaru, A. Samide, A. Moanță, C. Ionescu and C. Tigae, *Int. J. Electrochem. Sci.*, 10 (2015) 223.
23. A. Samide, B. Tutunaru, G. Bratulescu and C. Ionescu, *J. Appl. Polym. Sci.*, 130 (2013) 687.
24. A. Samide, B. Tutunaru, C. Ionescu and C. Tigae, *Int. J. Electrochem. Sci.*, 8 (2013) 3589.
25. A. Samide, B. Tutunaru, C. Negrila, I. Trandafir and A. Maxut, *Digest J. Nanomater. Biostruct.*, 6 (2011) 663.
26. A. Samide, B. Tutunaru, C. Tigae, R. Efrem, A. Moanta and M. Dragoi, *Environm. Protect. Eng.*, 2014 (2014) 93.
27. A. Samide, M. Dumitru, A. Ciuciu, B. Tutunaru and M. Preda, *Stud Univ. Babeş-Bolyai, Chemia*, 4 (2009) 157.
28. R. V. Khandare, A. N. Kabra, A. A. Kadam and S. P. Govindwar, *Int. Biodeter. Biodegr.*, 78 (2013) 89.
29. M. Mincea, V. Patrulea, A. Negrulescu, R. Szabo and V. Ostafe, *J. Water Resource Prot.*, 5 (2013) 446.
30. A. C. Gomes, J. C. Nunes and R. Simoes, *J. Hazard. Mater.*, 178 (2010) 57.
31. V. K. Gupta and R. Kumar, *Adv. Colloid Interface Sci.*, 193 (2013) 24.
32. M. Ghaedi, S. Hajati, B. Barazesh, F. Karimi and G. Ghezelbash, *J. Industrial Eng. Chem.*, 19 (2013) 227.
33. A. N. Ejhieh and H. Z. Mobarakeh, *J. Industrial Eng. Chem.*, 20 (2014) 1421.
34. K. Chaudhari, V. Bhatt, A. Bhargava and S. Seshadri, *Asian J. Water Environ. Pollut.*, 8 (2011) 127.
35. A. R. Khatee, A. Naseri, M. Zarei, M. Safarpour and L. Moradkhannejhad, *Environ. Tech.*, 33 (2012) 2305.
36. M. Punzi, B. Mattiasson and M. Jonstrup, *J. Photochem. Photobiol. A Chem.*, 248 (2012) 30.
37. M. E. Meibodi, M. R. Parsaeian and M. Banaei, *Ozone Sci. Eng.*, 35 (2013) 49.

38. M. A. Jayan, N. R. Maragatham and J. Saravanan, *Int. J. Appl. Bioeng.*, 5 (2011) 35.
39. M. Gonta, G. Duca, V. Matveevici, V. Iambartv and L. Mocanu, *Manage. Water Qual.*, 69 (2014) 197.
40. N. Djafarzadeh, M. Safarpour and A. Khataee, *Korean J. Chem. Eng.*, 31 (2014) 785.
41. E. Z. Godlewska, W. Przystas and E. G. Sota, *Water Air Soil Pollut.*, 225 (2014) 1.
42. S. B. Chergui, N. Oturan, H. Khalaf and M. A. Oturan, *Procedia Eng.*, 33 (2012) 181.
43. S. Shanthi and T. Mahalakshmi, *Int. J. Res. Pharm. Chem.*, 2 (2012) 289.
44. K. Chaudhari, V. Bhatt, A. Bhargava and S. Seshadri, *Asian J. Water Environ. Pollut.*, 8 (2011) 127.
45. H. Yilmaz, G. Ak and Ş. H. Şanlıer, *J. Biol. Chem.*, 40 (2012) 111.
46. K.-Y. Yeh, N. A. Restaino, M. R. Esopi, J. K. Maranas and M. J. Janik, *Catalysis Today*, 202 (2013) 20.
47. V. Climent, N. Garcia-Araez and J. M. Feliu, *Electroch. Commun.*, 8 (2006) 1577.
48. A. Lopez-Cudero, A. Cuesta and C. Gutierrez, *J. Electroanal. Chem.*, 586 (2006) 204.
49. D.-M. Zeng, Y.-X. Jiang, Z.-Y. Zhou, Z.-F. Su and S.-G. Sun, *Electrochim. Acta*, 55 (2010) 2065.
50. G. A. Attard and A. Brew, *J. Electroanal. Chem.*, 747 (2015) 123.
51. M. Inoue, A. Nakazawa and M. Umeda, *Int. J. Hydrogen Energy*, 37 (2012) 1226.
52. A. P. Yadav, A. Nishikata and T. Tsuru, *Electrochim. Acta*, 52 (2007) 7444.
53. G. Inzelt, B. B. Berkes, A. Kriston and A. Szekeley, *J. Solid State Electrochem.*, 15 (2011) 901.
54. X. Huang, Y. Qu, C. A. Cid, C. Finke, M. R. Hoffmann, K. Lim and S. C. Jiang, *Water Res.*, 92 (2016) 164.
55. M. Mastragostino and C. Gramellini, *Electrochim. Acta*, 30 (1985) 373.
56. A. R. Denaro, A. Mitchell and M. R. Richardson, *Electrochim Acta*, 16 (1971) 755.
57. A. Velikonja, E. Gongadze, V. Kralj-Iglic and A. Iglic, *Int. J. Electrochem. Sci.*, 9 (2014) 5885.
58. E. Gongadze, A. Velikonja, S. Perutkova, P. Kramar, A. Macek-Lebar, V. Kralj-Iglic and A. Iglic, *Electrochim. Acta*, 126 (2014) 42.
59. A. Khataee, V. Vatanpour and M. R. Farajzadeh, *Turkish J. Eng. Env. Sci.*, 32 (2008) 367.
60. V. Kostic, T. Stafilov and K. Stojanoski, *Sec. Math. Tech. Sci., MANU*, XXIX, 1–2 (2008) 89.
61. F. Gosetti, V. Gianotti, S. Angioi, S. Polati, E. Marengo and M.C. Gennaro, *J. Chromatogr. A*, 1054 (2004) 379.
62. A. Samide, B. Tutunaru, A. Moanta, C. Ionescu, C. Tigae and A. C. Vladu, *Int. J. Electrochem. Sci.*, 10 (2015) 4637.
63. A. Moanta, A. Samide, C. Ionescu, B. Tutunaru, A. Dobritescu, A. Fruchier and V. Barragan-Montero, *Int. J. Electrochem. Sci.*, 8 (2013) 780.